Using Viscosity Modifiers to Reduce Effective Diffusivity in Mortars

Kenneth A. Snyder[1]; Dale P. Bentz[2]; and Jeffrey M. Davis[3]

Abstract: Three viscosity modifiers (a commercial shrinkage-reducing admixture, a polypropylene glycol, and a cellulose ether) are used to reduce the effective diffusivity of chloride ions through mortars during a 1-year exposure. Two delivery mechanisms were studied: (1) adding a viscosity modifier to the mix water and (2) diluting the viscosity modifier in water, prewetting fine lightweight aggregate (LWA) with the solution, and replacing a portion of the sand with the prewetted LWA, which is equivalent to the practice of using LWA for internal curing. After a 28-day curing period, the cylinders were submerged in a 1- mol/L chloride solution. After 24 and 52 weeks of exposure, micro X-ray fluorescence analysis was used to profile the radial chloride concentration under ambient air pressure. The effective diffusivity was estimated by regression, assuming ideal Fickian radial diffusion. Compared with the control mortar (no admixture, no LWA), the addition of the viscosity modifier to the mix water reduced the effective diffusivity by nearly a factor of two, and using LWA saturated with a viscosity modifier reduced the effective diffusivity by a factor greater than two. Therefore, the use of these viscosity modifiers has the potential to double the service life of any concrete that may be subjected to degradation that depends on diffusion, such as corrosion of the steel reinforcement and sulfate attack. **DOI:** 10.1061/(ASCE)MT.1943-5533.0000524. *© 2012 American Society of Civil Engineers.*

CE Database subject headings: Diffusion; Curing; Aggregates; X rays; Mortars; Service life; Viscosity.

Author keywords: Diffusion; Internal curing; Lightweight aggregate; Micro X-ray fluorescence; Mortar; Service life; Viscosifier; Viscosity.

Introduction

In the 21st century, sustainability has emerged as a key concern of the construction community and society at large (Lippiatt 2007). A major contributor to the sustainability of a concrete structure is its service life, because when considered over a very long time, the environmental and economic effects are in proportion to the number of times the structure has to be repaired or replaced. In many degradation scenarios, including chloride-induced corrosion of steel reinforcement and external sulfate attack, the rate of diffusion of a deleterious species from the environment into the concrete largely controls its service life (Cusson et al. 2010). Conventionally, reduction of the effective diffusivity of these species in concrete is achieved by reducing the porosity and increasing the tortuosity of the hydrated cement paste through strategies such as reducing the water-to-cementitious materials ratio (w/cm) and/or adding supplementary cementitious materials. These approaches, however, may also increase the likelihood of early age cracking,

[1]Group Leader, Engineering Laboratory, National Institute of Standards and Technology, 100 Bureau Drive, Gaithersburg, MD 20899-8615 (corresponding author). E-mail: kenneth.snydernist.gov

[2]Chemical Engineer, Engineering Laboratory, National Institute of Standards and Technology, 100 Bureau Drive, Gaithersburg, MD 20899-8615. E-mail: dale.bentz@nist.gov

[3]Microscopist, Material Measurement Laboratory, National Institute of Standards and Technology, 100 Bureau Drive, Gaithersburg, MD 20899-8372. E-mail: jeff.davis@nist.gov

with these cracks providing preferential pathways for ion ingress [American Concrete Institute (ACI) 2010].

With this in mind, an alternate paradigm for decreasing effective diffusivity has been developed through the introduction of appropriate viscosity modifiers into the concrete pore solution (Bentz et al. 2008, 2009, 2010). These viscosifiers may be added directly to the mix water, in a manner equivalent to that employed for most conventional chemical admixtures, or a diluted solution of the viscosifier may be used to prewet fine lightweight aggregate (LWA). For the latter case, as the cement hydrates, this solution will be drawn out of the LWA into the surrounding cement paste owing to the chemical shrinkage and self-desiccation that accompanies cement hydration (Bentz 2005).

As this viscous solution is drawn from the LWA into the pore solution, the viscosity of the pore solution will increase. According to the Stokes-Einstein relation, the self-diffusion coefficient of an ion is inversely proportional to the viscosity (or hydrodynamic friction) of the solution in which it is diffusing; thus, doubling the viscosity of the pore solution should reduce the effective diffusivity by a factor of two (Shimizu and Kenndler 1999), in turn doubling the service life of the concrete in many degradation scenarios. This new technology for doubling concrete service life has been given the acronym VERDiCT: Viscosity Enhancers Reducing Diffusion in Concrete Technology (Bentz et al. 2009).

The objectives of this study are to extend the preliminary evaluations of VERDiCT in mortars (Bentz et al. 2010), by considering two water-to-cement mass ratios ($w/c = 0.4$ and 0.45) and three viscosifiers, and to obtain a more detailed quantitative analysis of the chloride ion profiles on the basis of micro X-ray fluorescence (μXRF). The latter allows a quantitative estimate of effective diffusivities to be obtained, including their uncertainties. In addition, thermogravimetric analysis (TGA) is used to examine the fate of the viscosifiers within the hydrated cement paste microstructure.

Materials and Experimental Procedures

An ASTM C150 (ASTM 2009) Type II/V low-alkali cement (that also qualifies as Type I) was employed in all mortar mixtures. It had a Blaine fineness of 387 m^2/kg, a density of 3,220 kg/m^3, and an ASTM C150–computed Bogue composition of 61% tricalcium silicate, 15% dicalcium silicate, 5% tricalcium aluminate, and 13% tetracalcium aluminoferrite by mass, with a sodium oxide equivalent of 0.31%. A mixture of four silica sands, each with a density of 2,610 kg/m^3, was used in each mortar. The fine LWA was a commercial expanded shale with a saturated surface dry (SSD) water absorption of 22% by mass at 25 °C and a measured water desorption of approximately 20% by mass at 25 °C when the SSD aggregates were exposed to a humid environment in equilibrium with a slurry of potassium nitrate (relative humidity of 93%). The measured SSD density was $1,800 \pm 50$ kg/m^3 (1 SD). For all mixtures, the total sand (normal + LWA) volume fraction was kept constant at 0.55, and the LWA was substituted for a similar size distribution of normal-weight sand on a volume basis.

Three viscosity modifiers were identified as having the potential to reduce the diffusivity of chloride ions: a polyoxyalkylene alkyl ether commercially available shrinkage-reducing admixture (denoted by the letter T), a polypropylene glycol with a molar mass of approximately 400 g/mol (P), and a high–molecular mass (> 10,000 g/mol) cellulose ether viscosifier (C). The expected effectiveness of each admixture was ascertained from solution conductivity measurements. The relative effect that an admixture (and its concentration) has on reducing the chloride diffusivity should be in proportion to the relative effect the admixture has on reducing the relative conductivity of potassium chloride solution. The details of this measurement process were described previously (Bentz et al. 2008). For this study, viscosifiers T and P were employed at a content equivalent to 10% (by mass) of the mix

solution (mix water + viscosifier), whereas C was used at a content equivalent to only 0.3% (by mass), because it is a much more effective viscosifier. At these concentrations, each viscosifier produced a solution with a viscosity approximately double that of water, and viscosifiers T and P significantly reduced the measured electrical conductivity of this solution, whereas viscosifier C increased it slightly.

Mortars were prepared at w/c of 0.40 and 0.45; their mixture designs are shown in Tables 1 and 2, respectively. In these tables, the sample name indicates the w/c, type of viscosifier used, and the delivery mechanism. The first two numbers indicate the w/c. The first letter for each mixture designates the composition of the mix water: W = distilled water (control), T = polyoxyalkylene alkyl ether in water P = polypropylene glycol in water,   and C = cellulose ether in water. The second letter indicates the presence or absence of LWA in the mixture: x = absent, and L = LWA is present. The third letter indicates the chemical solution used to prewet the LWA when it is present: x = LWA absent; W, T, or P = LWA is saturated with the viscosifier solution.

Tables 1 and 2 also include the estimated air content, as calculated by ASTM C185 (ASTM 2008), at the time of mixing. Most of these air content values range from 2–4%. The air content is greatest in the cellulose ether mixes, which suggests that this admixture may be acting as an air-entraining agent.

Mortars were prepared in a planetary mixer using the mixing procedures outlined in ASTM C305 (ASTM 2006). For each mortar mixture, 1250×100-mm mortar cylinders were cast and cured in sealed bags for 24 h. Mortars not containing LWA were demolded after 24 h and placed in a curing solution until an age of 28 d. This curing solution was prepared as a mixture of potassium, sodium, and calcium hydroxides. The concentration of hydroxides in each curing solution is shown in Table 3, and the values were chosen to approximately match the alkali composition of the mortar

Table 1. Mixture Designs for Mortar Mixtures with $w/c = 0.4$

Component	Wxx	Txx	Pxx	Cxx	WLW	WLT	WLP
Cement (g)	3,125	3,125	3,125	3,125	3,125	3,125	3,125
Mix water (g)	1,250	1,184	1,184	1,250	1,250	1,250	1,250
Sand (g)	7,006	7,209	7,209	7,006	5,247	5,247	5,247
Viscosifier in mix water (g)	0	132	132	4	0	0	0
Lightweight aggregate (g)	0	0	0	0	994	994	994
Water in lightweight aggregate (g)	0	0	0	0	219	80	80
Viscosifier in lightweight aggregate (g)	0	0	0	0	0	139	139
Air content (%)	1.42	2.16	2.93	4.84	3.46	3.85	3.70

Note: Air content is calculated using ASTM C185 (ASTM 2008) at the time of mixing.

Table 2. Mixture Designs for Mortar Mixtures with $w/c = 0.45$

Component	Wxx	Txx	Pxx	Cxx	WLW	WLT	WLP
Cement (g)	3,000	3,000	3,000	3,000	3,000	3,000	3,000
Mix water (g)	1,350	1,279	1,279	1,350	1,350	1,350	1,350
Sand (g)	7,182	7,095	7,095	7,182	5,206	5,206	5,206
Viscosifier in mix water (g)	0	142	142	4	0	0	0
Lightweight aggregate (g)	0	0	0	0	954	954	954
Water in lightweight aggregate (g)	0	0	0	0	210	60	60
Viscosifier in lightweight aggregate (g)	0	0	0	0	0	150	150
Air content (%)	1.92	0.44	2.07	6.03	2.17	3.68	4.16

Note: Air content is calculated using ASTM C185 (ASTM 2008) at the time of mixing.

Table 3. Concentration of Hydroxides in Curing Solutions Used for Mortars without Lightweight aggregate

Hydroxide	Concentration (mol/L)	
	$w/c = 0.40$	$w/c = 0.45$
Potassium hydroxide (KOH)	0.0948	0.0843
Sodium hydroxide (NaOH)	0.0178	0.0158
Calcium hydroxide [$Ca(OH)_2$]	0.0034	0.0040

specimens' internal pore solution. Mortars containing LWA were cured under sealed conditions by double wrapping them in two sealed plastic bags until an age of 28 d. Sealed curing was selected for these mixtures to promote the migration of the viscosifier/water solution from within the LWA into the surrounding hydrating cement paste (Bentz et al. 2010) and to mimic the conditions expected in the field.

At the end of each curing period, the mortar cylinders were each submerged in 600 mL of a 1- mol/L sodium chloride solution that was contained in a sealable plastic bottle. After exposure times of 24 and 52 weeks, sample cylinders were removed from their jars and evaluated for chloride penetration. At the designated exposure age, two cylinders were removed from their solution and split lengthwise using a universal testing machine. For each cylinder, one exposed surface was analyzed using μXRF; the relatively high sodium chloride concentration was chosen to ensure that the μXRF signal would be sufficient. Small fragments of some of the mortars were subjected to TGA by heating to a temperature of 1,000 °C at a heating rate of 10°C/ min.

Isothermal Calorimetry

A subset of the mortars was also evaluated for the influence of the viscosifiers on cement hydration rates using isothermal calorimetry. For each mortar mixture, two glass vials were loaded with approximately 8 g of fresh mortar and placed in the calorimeter, along with a reference vial containing dry cement powder. Heat release was then monitored to an age of 7 days. The results in Figs. 1(a) and 1(b) generally show a mild retardation owing to the presence of a viscosifier, with the exception of the cellulose ether that produced curves very similar to those of the control (no viscosifier) mixture. Introducing the viscosifier through the LWA, as opposed to through direct addition to the mixing water, reduced the effect of the retardation and increased the achieved hydration (particularly in the longer term for the $w/c = 0.4$ mortars). This increase in longer-term hydration has been noted previously for mortar mixtures with internal curing using LWA prewetted with only water (Bentz et al. 2010; Bentz 2009).

Micro X-Ray Fluorescence

Micro X-ray fluorescence (μXRF) has been used elsewhere to effectively track infiltrating ions in concrete (Davis et al. 2011). By exciting a polychromatic X-ray beam using a rhodium (Rh) target, the major and minor constituents of the cement paste and aggregate can be easily identified. Further more, by focusing the beam using a polycapillary optic, the beam spot can be manipulated to excite an area only 80 μm in diameter. The principal advantage to μXRF over other X-ray microanalytical techniques, such as scanning electron microscopy/electron probe X-ray microanalysis (SEM-EPMA) (Jensen et al. 1999), is the ability to extract elemental images from a heterogeneous surface at atmospheric pressure and without the same surface smoothness requirements as many other techniques.
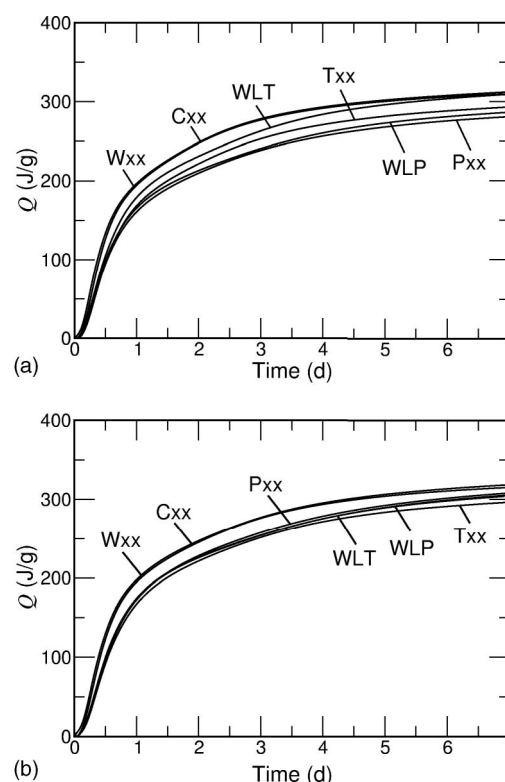
Fig. 1. Cumulative heat release Q, per gram of cement, up to 7-day hydration for mortar mixtures: (a) $w/c = 0.4$; (b) $w/c = 0.45$

Early experiments designed to optimize the measurement protocol revealed that certain considerations were necessary to ensure accurate, reliable measurements. First, applying a vacuum to the system, which improves the detection sensitivity to light elements, tends to dry out the concrete specimen and force chloride ions further into the specimen. Because μXRF is a surface technique, removal of ions from the surface will severely affect the results. Second, because the system uses polychromatic Rh radiation, the Rh $L\alpha$ X-ray line will overlap with the chlorine (Cl) $K\alpha$ X-ray line, significantly increasing the lower limit of detection for Cl and making the background very difficult to model. A 25-μm thick aluminum (Al) foil was used to prevent the Rh $L\alpha$ radiation from reaching the sample, thereby eliminating the Rayleigh scatter Rh peak from the spectrum. The effective background in the Cl region is very low with the Al foil in place. Finally, although μXRF is not as sensitive to surface roughness as electron microscope–based techniques, some consideration is required to produce high-quality images and spectra. Random roughness induced by breaking the cylinder was on the order of 0.5 mm over a field of view, although global variations in the surface could be several millimeters. Careful visual inspection of the surface was necessary to mark out an area with no major variations for analysis. Each field of view was sufficiently large to include a large number of aggregates, thus ensuring a representative sample.

Given the considerations mentioned, the optimal measurement protocol was as follows: The samples were imaged using a point-to-point distance of 80 μm in both the z (longitudinal) and r (radial) directions, typically with 200 points in the z direction and 300 points in the r direction. At each measurement point, a full X-ray spectrum up to 10 keV was acquired for 1 s using a Si (Li) detector on an energy dispersive spectrometer (EDS) with a resolution of 165 eV at 5.9 keV. The X-ray data were stored in a binary database, which was later interrogated with NIST

developed Lispix software (Bright 2000). Each measurement took approximately 18 h and was typically run overnight. Samples were measured at atmospheric pressure and ambient temperature for all experiments.

Effective Diffusivity

The effective chloride diffusivity for each cylinder was estimated by assuming ideal radial Fickian diffusion in a cylindrical coordinate system. The concentration at radial position r and time t for a cylinder having radius R, an initial internal background concentration C_b, and in contact with a constant concentration C_s at the surface, can be expressed analytically (Crank 1975, Eq. 5.22)

$$\frac{C(r,t) - C_b}{C_s - C_b} = 1 - \frac{2}{R}\sum_{n=1}^{\infty}\frac{\exp(-\alpha_n^2 Dt)J_o(\alpha_n r)}{\alpha_n J_1(\alpha_r r)} \quad (1)$$

It is assumed that the external concentration of chloride is constant, because the 600 mL of available solution provides a large (nearly constant) reservoir of chloride ions. The parameter D is the Fickian diffusivity of the species of interest. The quantities are the Bessel functions of first kind having orders of zero and one, respectively (Abramowitz and Stegun 1972). Each value of satisfies the positive roots of the following equation:

$$J_o(\alpha_n R) = 0 \quad (2)$$

It is assumed that the μXRF chloride count is proportional to the concentration of chloride ions. Therefore, the μXRF counts are surrogates for concentration, and Eq. (1) has three unknown parameters: the Fickian diffusivity D, the background counts C_b, and the surface counts C_s. Even though only three adjustable parameters and hundreds of measurements exist, the estimated result for D at early ages can depend strongly on the estimated background value is available.

Fortunately, an independent means of estimating the background value is available. Before each measurement, the X-ray flux was adjusted to a constant value using a standard target. Given that the aggregate fraction was kept constant and that the cement paste microstructures were similar for all specimens, it would be a reasonable estimate to assume that the chloride background count for all specimens at the same age of chloride exposure would be approximately constant. From a spectral analysis of the detected X-rays, it is possible to determine the fraction of counts to be attributed to the chloride peak and the remaining fraction that should be attributed to the background. Although this doesn't indicate which counts are attributed to chlorides and which are attributed to the background, it is an indication of the number fraction that should be attributed to the background.

Assuming that these background counts are randomly distributed uniformly across the entire image, it is possible to estimate the average background value that should be attributed to each pixel in the image, thus yielding the background value C_b. Taking the values from all the specimens at a given age provided a means of estimating the uncertainty (expressed as the estimated standard deviation). At 24 weeks, the estimated average background was 8.22 ± 0.29, and at 52 weeks, this value was 9.03 ± 0.31; the reported uncertainty is the standard deviation of the population and indicates the relatively constant values observed throughout the study.

The outputs from the μXRF measurements were two-dimensional images of the sample, with the intensity representing the signal strength for a particular element. Fig. 2 shows typical element images (for mortar sample 40WLT-3 after 24 weeks of chloride exposure) for calcium [Figs. 2(a) and 2(d)], silicon [Figs. 2(b) and 2(e)], and Cl [Figs. 2(c) and 2(f)], along with a graph showing the average number of counts in each column. The data begin 250 μm from the outside surface because of the signal fall-off at the edge of the sample. The Cl profile indicates that the background value is less than the value of 8.22 from the spectral analysis. Closer comparison of the elemental maps shows that neither the (silica-rich) sand nor the LWA (medium gray in the silicon map) contributes to the chloride map. Therefore, the spectral analysis considers only those pixels that contribute counts to the chloride map, which does not include either aggregate. This
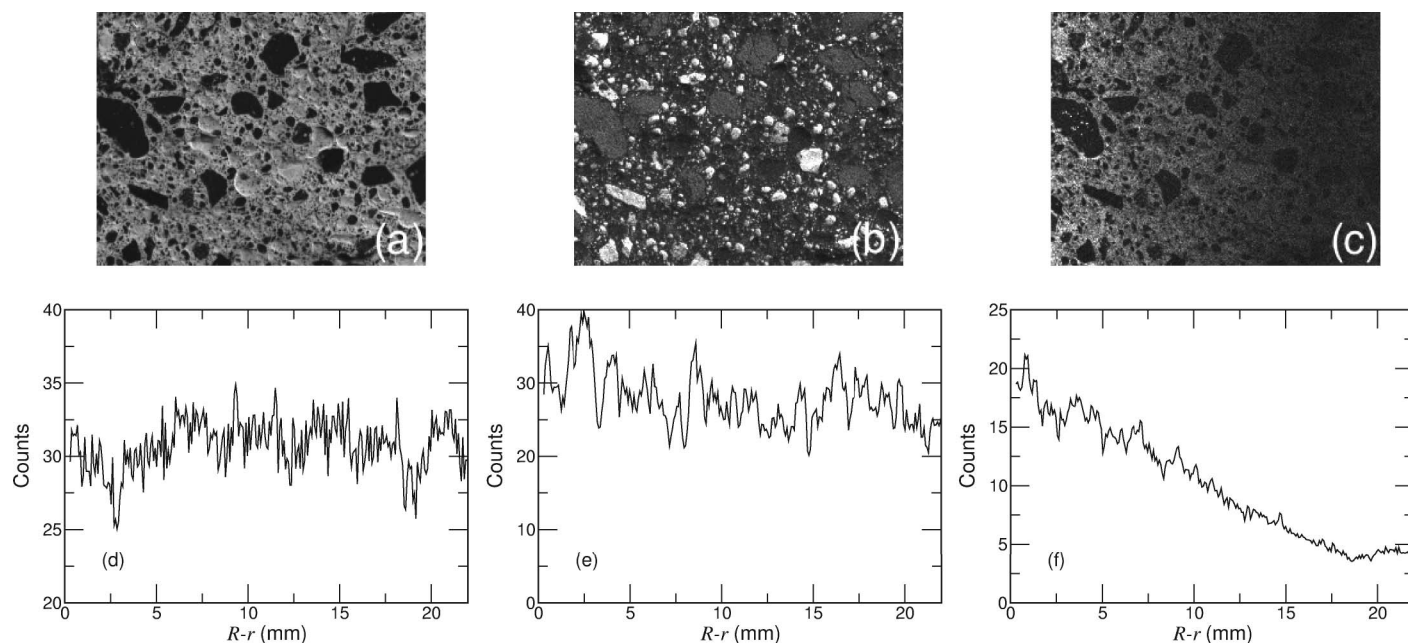
Fig. 2. Image maps (22.0-mm wide, 17.0-mm high) for sample 40WLT-3 after 24 weeks of exposure: (a) calcium; (b) silicon; (c) chlorine (the sample surface is 250 μm beyond the left side of each image); plots of the average intensity for each column of pixels: (c) calcium; (e) silicon; and (f) chlorine

means that the estimated chloride background is the paste fraction (0.45) times the previous background values: 3.70 at 24 weeks and 4.06 at 52 weeks. Because this approach is still an approximation, the uncertainty attributed to both of these values is 1.0, representing 1 SD.

An estimate for the uncertainty in the background value provided a means of estimating the uncertainty in the diffusivity D. For a fixed background value C_b, it is possible to perform a two-parameter regression to find best estimates for D and C_o. Because uncertainty in the estimated background is quantified, a population of D values is obtained by sampling over the distribution for C_b. Fig. 3 shows the outcome of the analysis performed for the sample shown in Fig. 2. The horizontal dashed line denotes the estimated background value of 3.70, and the Gaussian curve denotes the uncertainty (1 SD) in this value. Repeatedly performing the regression using samples from the Gaussian curve for the background yields a distribution of diffusivities (D), surface concentrations (C_o), and profiles. The three smooth curves in Fig. 3 represent the population of profiles: the middle curve is the average, and the upper and lower curves represent the 95th percentiles of the population of curves recorded at the value of $R - r$.

To make a quantitative statement about the expanded uncertainty (Taylor and Kuyatt 1993) in the reported value of Dt/R^2, it is necessary to ascertain the probability distribution function of the population of values. Because the values of C_b were normally distributed, the assumption was that the values of Dt/R^2 would also be normally distributed. The calculated values of Dt/R^2 from the regression results in Fig. 3 are shown as filled circles in Fig. 4. The x-value is the calculated parameter from the regression, and the y-value is the cumulative probability of the corresponding measured values. The mean ($+/- 1$SD) of the values was 0.0653 ± 0.0092. The smooth curve in the figure is the normal probability function for a distribution with the same mean and standard deviation. As shown in the figure, the population of Dt/R^2 values is approximated reasonably well by a normal distribution. Therefore, the coverage factor of the reported standard deviations is approximately equivalent to that for 1 SD of a normal distribution.

Results and Discussion

At the prescribed time of exposure, two cylinders were removed from their container, towel dried, split in two longitudinally, and sealed in a jar until the measurement was made (within 4 days of splitting); one chloride profile was made from each of the
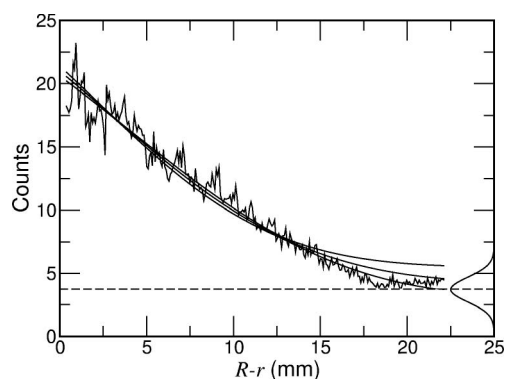
Fig. 3. Scaled chloride profile, expressed as a function of the radial distance r, in a cylinder having radius R
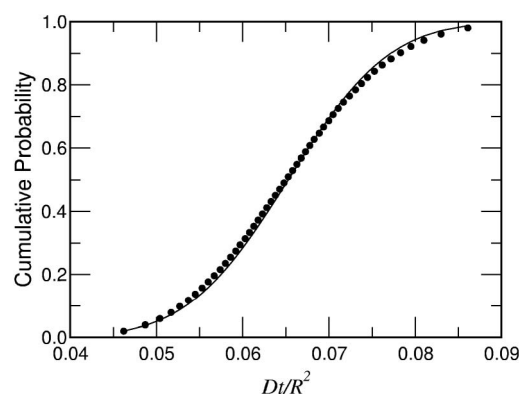
Fig. 4. Measured and estimated probability function for values of Dt/R^2 calculated for sample 40WLT-3

two cylinders. In some cases, either instrumentation or scheduling problems allowed for only a single chloride profile.

Mass Change

The mass of each cylinder (SSD) was determined before exposure to chloride solution and again just before splitting. The mass increase between the time of exposure and the time of testing is shown in Table 4, in which the change is expressed as a percentage. The data indicate that the cylinders continued to absorb liquid between 24 and 52 weeks of exposure. These data reveal two noteworthy facts: the presence of VERDiCT and LWA appear to have a greater influence on the mass change than the w/c binder ratio; and the minor mass increase for the cellulose ether (Cxx) mixes, which had the greatest air content, suggests that the air voids in these systems are no more saturated than in the Wxx specimens.

Surface Concentration

The variability of the estimated surface concentration C_s is an indication of the uniformity among the samples and the measurement process. The estimated C_s values are shown in Table 5. Although the values increase slightly 24- to 52-weeks' exposure, the values

Table 4. Cylinder Mass Increase Between Beginning of Chloride Exposure and Time of Testing

	Mass increase (%)	
Mixture	At 24 weeks	At 52 weeks
40Wxx	0.17, 0.21	0.30, 0.30
40Txx	0.52, 0.46	0.69, 0.78
40Pxx	0.59, 0.64	0.84, 0.85
40Cxx	0.21, 0.26	0.39, 0.34
40WLW	0.51, 0.55	0.69, 0.74
40WLT	1.18, 1.22	1.55, 1.55
40WLP	1.59, 1.69	2.26, 2.30
45Wxx	0.21, 0.13	0.30, 0.30
45Txx	0.47, 0.47	0.61, 0.63
45Pxx	0.60, 0.64	0.77, 0.68
45Cxx	0.26, 0.27	0.40, 0.40
45WLW	0.78, 0.82	1.01, 0.94
45WLT	1.41, 1.47	1.71, 1.79
45WLP	1.95, 2.01	2.65, 2.34

Note: Two values were determined for each mixture at each exposure time.

Table 5. Mean Values of Surface Concentration C_s (Chloride Counts) for $w/c = 0.40$ and 0.45 Samples

Mixture	Surface concentration C_s	
	At 24 weeks	At 52 weeks
40Wxx	34.68 ± 0.05	39.06 ± 0.01; 42.49 ± 0.00
40Txx	36.52 ± 0.19	46.60 ± 0.04; 37.55 ± 0.01
40Pxx	33.40 ± 0.16; 35.13 ± 0.11	41.37 ± 0.01
40Cxx	22.40 ± 0.06; 32.40 ± 0.05	42.26 ± 0.00; 38.54 ± 0.00
40WLW	29.88 ± 0.09	42.22 ± 0.01
40WLT	20.99 ± 0.20; 25.62 ± 0.27	39.02 ± 0.04; 47.61 ± 0.07
40WLP	31.15 ± 0.17; 39.08 ± 0.12	45.63 ± 0.02
45Wxx	33.63 ± 0.00; 33.58 ± 0.03	41.30 ± 0.00; 43.81 ± 0.00
45Txx	35.06 ± 0.11; 34.48 ± 0.07	40.50 ± 0.00; 41.94 ± 0.01
45Pxx	23.73 ± 0.02; 36.36 ± 0.03	41.30 ± 0.00; 38.33 ± 0.00
45Cxx	29.34 ± 0.00; 30.68 ± 0.00	—
45WLW	35.89 ± 0.02	40.27 ± 0.00
45WLT	27.01 ± 0.08; 28.74 ± 0.21	42.15 ± 0.03
45WLP	26.74 ± 0.06; 32.35 ± 0.13	—

Note: The reported uncertainty is the population standard deviation of the C_s values from the Monte Carlo calculation. In some cases, only one measurement was possible. For the two cases of unreported values, the chloride ingress was so severe that an estimate was not possible.

are relatively constant among samples of the same exposure, regardless of w/c value. For the two instances of no reported values, the penetration was so significant that a determination of C_s was not possible.

Fickian Diffusivity

The Fickian diffusion coefficient is the primary material parameter that, along with the sample geometry, determines the time span before the onset of degradation. Because these mortars do not represent concrete, the specific values of diffusivity are not important. Instead, the dimensionless quantity Dt/R^2 is convenient because it yields a number having a magnitude near one, and it can be converted to diffusivity using the cylinder radius R and the exposure time t.

The estimated values of the dimensionless parameter Dt/R^2 for each observed cylinder are shown in Table 6. The values in parentheses denote the average and standard deviation of the Dt/R^2 values, as calculated from the regression calculations. For the two instances of no reported values, the penetration was so significant that a determination of Dt/R^2 was not possible.

For the entries in Table 6 that consist of two measurements, a single expression for Dt/R^2 can be obtained by calculating the average and propagating the errors. The resulting values are shown in Table 7. This condensed representation facilitates a direct comparison between pairs of specimens. The values of Dt/R^2 approximately double, as they shoule, between 24 and 52 weeks. This suggests that the chlorides are being transported primarily by Fickian diffusion; relatively little binding, absorption, or reaction occurs during this time period. The notable exception to this is the 45WLW specimens, which are discussed subsequently.

The performance of any given approach for reducing the diffusion coefficient can be characterized by the ratio of its Dt/R^2 value to the value for that of the ordinary portland cement (OPC) mortar (Wxx). Because the measurements were made at the same time, and because the cylinder radii are constant, these ratios represent the ratio of Fickian diffusivities. These ratios for $w/c = 0.40$ and 0.45 are shown separately in Figs. 5(a) and 5(b). In both cases, the

Table 6. Estimated Values of Dimensionless Parameter Dt/R^2 from each Observed Cylinder

| Mixture	Dt/R^2	
	At 24 weeks	At 52 weeks
40Wxx	0.1130 ± 0.0054	0.1979 ± 0.0047; 0.2840 ± 0.0042
40Txx	0.0819 ± 0.0055	0.1348 ± 0.0040; 0.1880 ± 0.0050
40Pxx	0.0856 ± 0.0061; 0.0888 ± 0.0054	0.1881 ± 0.0044
40Cxx	0.0994 ± 0.0088; 0.1060 ± 0.0058	0.2044 ± 0.0043; 0.2501 ± 0.0047
40WLW	0.1023 ± 0.0067	0.1951 ± 0.0043
40WLT	0.0653 ± 0.0092; 0.0623 ± 0.0077	0.1335 ± 0.0049; 0.1290 ± 0.0041
40WLP	0.0847 ± 0.0065; 0.0912 ± 0.0049	0.1689 ± 0.0040
45Wxx	0.1955 ± 0.0054; 0.1503 ± 0.0056	0.4077 ± 0.0043; 0.3620 ± 0.0041
45Txx	0.1109 ± 0.0058; 0.1199 ± 0.0057	0.2659 ± 0.0045; 0.2243 ± 0.0043
45Pxx	0.1568 ± 0.0084; 0.1331 ± 0.0051	0.2541 ± 0.0044; 0.2412 ± 0.0048
45Cxx	0.2213 ± 0.0064; 0.2090 ± 0.0060	—
45WLW	0.1723 ± 0.0052	0.5244 ± 0.0045
45WLT	0.1111 ± 0.0076; 0.0871 ± 0.0076	0.1607 ± 0.0045
45WLP	0.1154 ± 0.0075; 0.0965 ± 0.0062	—

Note: The reported uncertainty is the population standard deviation of the Dt/R^2 values from the Monte Carlo calculation. In some cases, only one sample was analyzed. For the two cases of unreported values, the chloride ingress was so severe that an estimate was not possible.

Table 7. Estimated Values of Dt/R^2 (Using Average Values from Table 6) with Uncertainty (1 SD) Representing Propagation of Errors

Mixture	Dt/R^2	
	At 24 weeks	At 52 weeks
40Wxx	0.1130 ± 0.0054	0.2410 ± 0.0032
40Txx	0.0819 ± 0.0055	0.1614 ± 0.0032
40Pxx	0.0872 ± 0.0041	0.1881 ± 0.0044
40Cxx	0.1027 ± 0.0053	0.2273 ± 0.0032
40WLW	0.1023 ± 0.0067	0.1951 ± 0.0043
40WLT	0.0638 ± 0.0060	0.1313 ± 0.0032
40WLP	0.0880 ± 0.0041	0.1689 ± 0.0040
45Wxx	0.1729 ± 0.0039	0.3849 ± 0.0030
45Txx	0.1154 ± 0.0041	0.2451 ± 0.0031
45Pxx	0.1450 ± 0.0049	0.2477 ± 0.0033
45Cxx	0.2090 ± 0.0044	—
45WLW	0.1723 ± 0.0052	0.5244 ± 0.0045
45WLT	0.0991 ± 0.0054	0.1607 ± 0.0045
45WLP	0.1060 ± 0.0049	—

WLT specimens had the lowest relative diffusivities, with the effectiveness increasing over time. For the $w/c = 0.45$ mortars, the WLT mortar had a diffusivity that was less than half that of
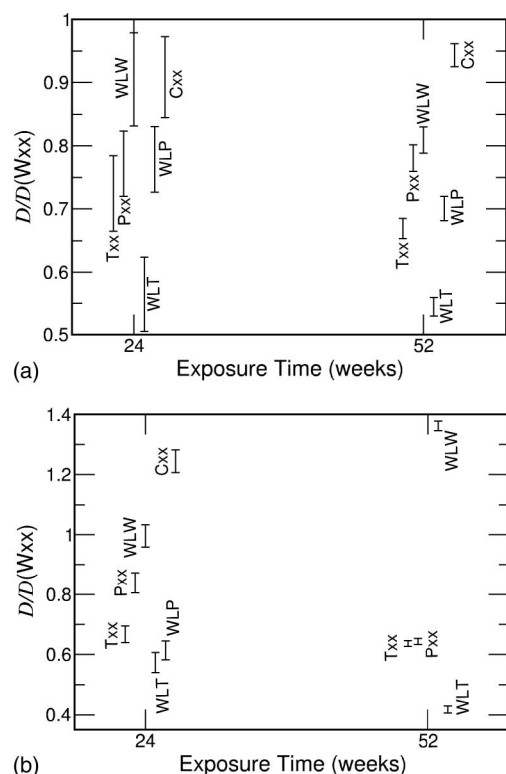
Fig. 5. Ratio of estimated diffusivity D to diffusivity $D(Wxx)$ estimated for Wxx sample of same w/c ratio and exposure time: (a) $w/c = 0.40$ mortars; (b) $w/c = 0.45$ mortars

the Wxx mortar after 52 weeks of exposure to a chloride solution. Therefore, the expected service life of the WLT mortar, in an environment in which diffusion was the controlling transport mechanism, would be twice that of the Wxx mortar.

The effectiveness of saturated LWA seems to depend on the w/c value and the use of a viscosifier. For the $w/c = 0.40$ mortars, LWA improved performance, with the addition of a viscosifier having a positive effect. For the $w/c = 0.45$ mortars, however, water-filled LWA (WLW) had higher diffusivities than the Wxx mortar, and the polypropylene-filled LWA (WLP) had an even higher diffusivity; the chloride profile for the WLP specimen was nearly horizontal.

A review of the mass change data in Table 4 suggests that absorption of the chloride solution by LWA does not provide a comprehensive explanation for the behavior. The WLT samples had the smallest effective chloride diffusivities, yet they also had the second greatest mass increases at both exposure times and both w/c values. Although water content plays an important role in providing pathways for diffusion, so does the connectivity of the pore structure. It would appear that the role that water plays in changing the microstructure of the mortars owing to hydration has a greater effect on the diffusivity than merely the total quantity of water.
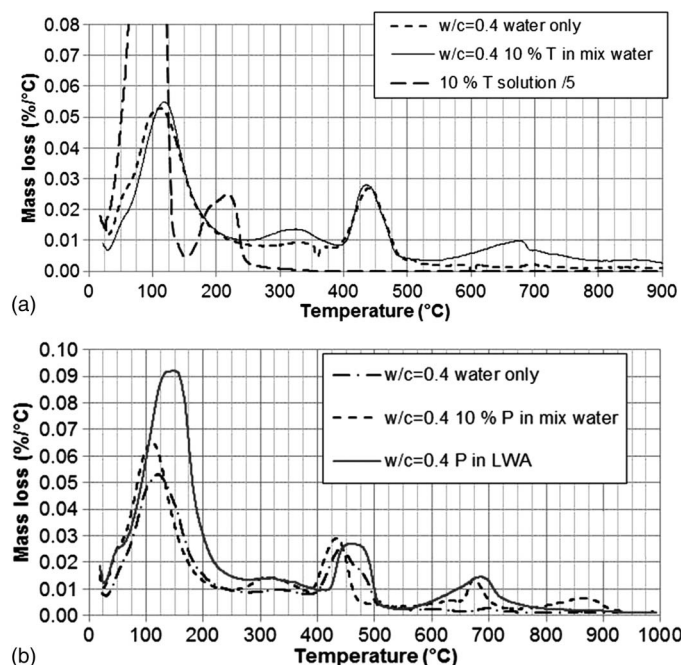
Thermogravimetric Analysis

Thermogravimetric analysis (TGA) was applied to investigate the fate of two of the viscosifiers (T and P) within the hydrating cement paste microstructure. Specifically, TGA of the external exposure solution was used to examine whether significant leaching of the viscosifier from the specimen into the exposure environment occurs, and TGA of broken mortar fragments was used to infer the incorporation of the viscosifier into the cement hydration

products (Beaudoin et al. 2008). Results are shown in Figs. 6, 7(a), and 7(b). The curves in Fig. 6 are the TGA curves for various solutions, indicating that little if any of viscosifier T is present in the 1-year exposure solution, because the TGA curve for the 1-year exposure solution is basically identical to that of a freshly prepared 1- mol/L solution of chloride ions, with a peak greater than 800°C owing to the presence of the chlorides and containing no peaks in the temperature range of 150–300°C, which would be indicative of the presence of the viscosifier. Similar curves (not shown) were obtained for viscosifier P. Minimal leaching of the viscosifier into the exposure environment is one requirement for the successful long-term performance of VERDiCT in field concrete.

Fig. 7 shows that viscosifiers T [Fig. 7(a)] and P [Fig. 7(b)] are likely bound, either physically or chemically, within the structure of the cement hydration products, because the two viscosifiers are not volatilized until much higher temperatures in the mortar specimens, compared with the TGA scans for the solutions. The incorporation
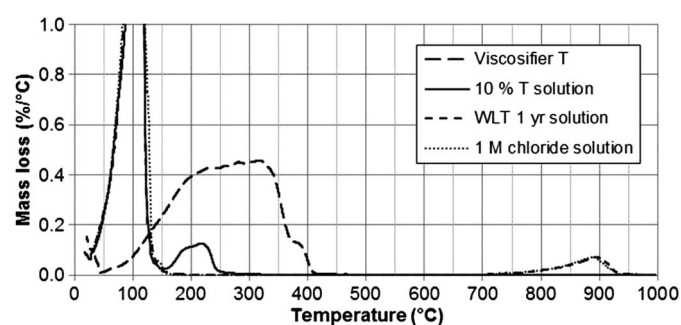
Fig. 6. Thermogravimetric analysis scans for different solutions

Fig. 7. Thermogravimetric analysis scans for mortar specimens and solutions: (a) viscosifier T; (b) viscosifier P; the peak observed at greater than 800°C for the 10% P in mix water curve is likely owing to the presence of chlorides (Fig. 6)

of polyethylene glycols (somewhat similar in chemical structure to viscosifiers *T* and *P*) into the structure of calcium silicate hydrate has been observed by Beaudoin et al. (2008). This would be consistent with the minimal leaching observed for these viscosifiers. The successful performance of these molecules as effective reducers of diffusivities indicates that such incorporation into the hydration products does not adversely limit their effectiveness in this role.

Conclusions

In this study, OPC mortars having w/c mass ratios of 0.40 and 0.45 have been used to demonstrate that the use of viscosity modifiers can successfully reduce the effective diffusivity of chloride ions. After 24 and 52 weeks of submerged exposure to a chloride solution, an analysis of the μXRF profile of Cl indicates that the effective diffusivity of mortars containing LWA saturated with a viscosity modifier can be reduced to approximately one-half the value for a mortar without either LWA or a viscosity modifier. Analysis of the predicted surface concentrations indicates that the measurement technique was consistent over all the samples, and TGA of the chloride solution and the mortar indicates that the viscosifiers are remaining inside the cement paste.

The approach of using viscosity modifiers to reduce diffusion, demonstrated in mortars in this study, may provide an alternative method for dramatically increasing the service life of a concrete subjected to diffusion-controlled degradation (e.g., rebar corrosion, sulfate attack). Further testing on typical concrete formulations is needed to confirm that the viscosifier delivery methods are practical and that the performance thus far is not an artifact of testing on mortars.

Acknowledgments

References

Abramowitz, M., and Stegun, I. A. (1972). *Handbook of mathematical functions*, Dover Publications, New York.

American Concrete Institute (ACI). (2010). "Report on early-age cracking: Causes, measurement, and mitigation." *ACI 231R-10*, ACI, Detroit.

ASTM. (2006). "Standard practice for mechanical mixing of hydraulic cement pastes and mortars of plastic consistency." *ASTM C305*, West Conshohocken, PA.

ASTM. (2008). "Standard test method for air content of hydraulic cement mortar." *ASTM C185*, West Conshohocken, PA.

ASTM. (2009). "Standard specification for portland cement." *ASTM C150*, West Conshohocken, PA.

Beaudoin, J. J., Drame, H., Raki, L., and Alizadeh, R. (2008). "Formation and properties of C-S-H-PEG nanostructures." *Mater. Struct.*, 42(7), 1003–1014.

Bentz, D. P. (2005). "Capitalizing on self-desiccation for autogenous distribution of chemical admixtures in concrete." *Proc., 4th Int. Seminar on Self-Desiccation and Its Importance in Concrete Technology*, B. Persson, D. Bentz, and L.-O. Nilsson, eds., Lund Univ., Lund, Sweden, 189–196.

Bentz, D. P. (2009) "Influence of internal curing using lightweight aggregates on interfacial transition zone percolation and chloride ingress in mortars." *Cem. Concr. Compos.*, 31(5), 285–289.

Bentz, D. P., Peltz, M. A., Snyder, K. A., and Davis, J. M. (2009). "VERDiCT: Viscosity Enhancers Reducing Diffusion in Concrete Technology." *Concr. Int.*, 31(1), 31–36.

Bentz, D. P., Snyder, K. A., Cass, L. C., and Peltz, M. A. (2008). "Doubling the service life of concrete. I: Reducing ion mobility using nanoscale viscosity modifiers." *Cem. Concr. Compos.*, 30(8), 674–678.

Bentz, D. P., Snyder, K. A., and Peltz, M. A. (2010). "Doubling the service life of concrete structures. II: Performance of nanoscale viscosity modifiers in mortars." *Cem. Concr. Compos.*, 32(3), 187–193.

Bright, D. (2000). "Lispix: Image processing and data visualization tool for the PC and macintosh." *Scanning*, 22(2), 111–112.

Crank, J. (1975). *The mathematics of diffusion*, 2nd Ed., Oxford Science Publications, Oxford, U.K.

Cusson, D., Lounis, Z., and Daigle, L. (2010). "Benefits of internal curing on service life and life-cycle cost of high-performance concrete bridge decks: A case study." *Cem. Concr. Compos.*, 32(5), 339–350.

Davis, J. M., Newbury, D. E., Ritchie, N. W. M.Vincenzi, E., and Bentz, D. (2011). "Bridging the micro-to-macro gap: A new application for micro X-ray fluorescence." *Microsc. Microanal.*, 17(3), 410–417.

Jensen, O. M., Hansen, P.-F., Coats, A. M., and Glasser, F. P. (1999). "Chloride ingress in cement paste and mortar." *Cem. Concr. Res.*, 29(9), 1497–1504.

Lippiatt, B. C. (2007). "BEES 4.0 building for environmental and economic sustainability technical manual and user guide." *NIST Internal Rep. 7423*, National Institute of Standards and Technology, U.S. Dept. of Commerce, Washington, DC.

Shimizu, T., and Kenndler, E. (1999). "Capillary electrophoresis of small solutes in linear polymer solutions: Relation between ionic mobility, diffusion coefficient, and viscosity." *Electrophoresis*, 20(17), 3364–3372.

Taylor, B. N., and Kuyatt, C. E. (1993). "Guidelines for evaluating and expressing the uncertainty of NIST measurement results." *NIST Technical Note 1297*, National Institute of Standards and Technology, U.S. Dept. of Commerce, Washington, DC.